Biochimica et Biophysica Acta 1827 (2013) 1031–1038

Contents lists available at SciVerse ScienceDirect

Biochimica et Biophysica Acta

journal homepage: www.elsevier.com/locate/bbabio

Review

Interconversion of CO_2 and formic acid by bio-inspired Ir complexes with pendent bases ☆

Etsuko Fujita [a,*], James T. Muckerman [a], Yuichiro Himeda [b]

[a] Chemistry Department, Brookhaven National Laboratory, Upton, NY 11973-5000, USA
[b] National Institute of Advanced Industrial Science and Technology, Tsukuba Central 5-2, 1-1-1 Higashi, Tsukuba, Ibaraki 305-8565, Japan

ARTICLE INFO

Article history:
Received 1 October 2012
Received in revised form 8 November 2012
Accepted 10 November 2012
Available online 19 November 2012

Keywords:
CO_2 hydrogenation
Formic acid
Dehydrogenation
Ir complexes
H_2 storage
Bio-inspired catalysts

ABSTRACT

Recent investigations of the interconversion of CO_2 and formic acid using Ru, Ir and Fe complexes are summarized in this review. During the past several years, both the reaction rates and catalyst stabilities have been significantly improved. Remarkably, the interconversion (i.e., reversibility) has also been achieved under mild conditions in environmentally benign water solvent by slightly changing the pH of the aqueous solution. Only a few catalysts seem to reflect a bio-inspired design such as the use of proton responsive ligands, ligands with pendent bases or acids for a second-coordination-sphere interaction, electroresponsive ligands, and/or ligands having a hydrogen bonding function with a solvent molecule or an added reagent. The most successful of these is an iridium dinuclear complex catalyst that at least has the first three of these characteristics associated with its bridging ligand. By utilizing an acid/base equilibrium for proton removal, the ligand becomes a strong electron donor, resulting in Ir(I) character with a vacant coordination site at each metal center in slightly basic solution. Complemented by DFT calculations, kinetic studies of the rates of formate production using a related family of Ir complexes with and without such functions on the ligand reveal that the rate-determining step for the CO_2 hydrogenation is likely to be H_2 addition through heterolytic cleavage involving a "proton relay" through the pendent base. The dehydrogenation of formic acid, owing to the proton responsive ligands changing character under slightly acidic pH conditions, is likely to occur by a mechanism with a different rate-determining step. This article is part of a Special Issue entitled: Metals in Bioenergetics and Biomimetics Systems.

1. Introduction

Formate dehydrogenases are enzymes that catalyze oxidation of formate to CO_2. The most common class of the enzymes directly transfers a hydride moiety from formate to $NADP^+$, however, the reverse reaction is difficult to drive because the reduction potential of $NADP^+$ is more positive than that of CO_2 [1]. The formate dehydrogenases that contain molybdenum or tungsten cofactors can transfer an electron from formate to reduce quinone, protons, or $NADP^+$, therefore formate becomes CO_2 and H^+. In fact, interconversion of CO_2 and formate is essential to the metabolism of several bacteria. Formate is a common growth substrate and also functions as an accessory reductant for the utilization of more complex substrates, and an intermediate in energy-conserving pathways [2]. Reda et al. demonstrated reversible interconversion of CO_2 and formate using tungsten-containing formate dehydrogenase enzyme immobilized on an electrode surface [1]. They found that it catalyzes efficient electrochemical reduction of CO_2 to formate with a rate more than two orders of magnitude faster than any known catalysts for the same reaction. Electrochemical formate oxidation ($3380\ s^{-1}$ at pH 8) is much faster than CO_2 reduction ($280\ s^{-1}$ at pH 7.5) [1]. Unfortunately the structure of the enzyme they used is not known, however, structures of several molybdenum or tungsten containing enzymes have been determined. In the active site, molybdenum or tungsten is coordinated to the *cis*-dithiolene group of one or two pyranopterins in addition to terminal oxo/hydroxo groups and/or sulfido groups or side chains of serine, cysteine, selenocysteine or aspartate residues in a diversity of arrangements [3]. For CO_2-formate conversion, the arginine residue is proposed to orient CO_2 and formate suitably for proton delivery and removal, respectively, via hydrogen-bonding interactions with a histidine residue in the active site.

While biological systems do not directly utilize dihydrogen for formate synthesis from CO_2, bio-inspired artificial systems for the interconversion of CO_2 and formate are of interest [4–6]. CO_2 hydrogenation in water is rather complicated owing to the acid/base equilibrium of CO_2 as shown in Eq. (1). Although the hydrogenation of CO_2 into formic acid (Eq. (2)) in the gas phase is endergonic ($\Delta G^\circ_{298} = +33$ kJ mol^{-1}), the reaction in the aqueous phase is exergonic ($\Delta G^\circ_{298} = -4$ kJ mol^{-1}) and the presence of a base makes the hydrogenation of CO_2 more favorable [7,8]. Similarly, on the basis of theoretical calculations, the

---

☆ This article is part of a Special Issue entitled: Metals in Bioenergetics and Biomimetics Systems.

* Corresponding author. Tel.: +1 631 344 4356; fax: +1 631 344 5815.
E-mail address: fujita@bnl.gov (E. Fujita).

0005-2728/$ – see front matter © 2012 Elsevier B.V. All rights reserved.
http://dx.doi.org/10.1016/j.bbabio.2012.11.004

hydrogenation of bicarbonate into formate in water (Eq. (3)) is believed to be exergonic. Formate is the conjugate base of formic acid (Eq. (4)) and the dehydrogenation is more favorable in acidic conditions.

$$CO_2 + H_2O \rightleftharpoons H_2CO_3 \overset{pK_1=6.35}{\rightleftharpoons} HCO_3^{\ -} + H^+ \overset{pK_2=10.33}{\rightleftharpoons} CO_3^{\ 2-} + 2H^+ \tag{1}$$

$$CO_2 + H_2 \rightleftharpoons HCO_2H \tag{2}$$

$$HCO_3^{\ -} + H_2 \rightleftharpoons HCO_2^{\ -} + H_2O \tag{3}$$

$$HCO_2H \overset{pK_a=3.75}{\rightleftharpoons} HCO_2^{\ -} + H^+ \tag{4}$$

In this article, we will review recent investigations of homogeneous catalytic hydrogenation of CO_2 to formate and dehydrogenation of formic acid in various solvents including water. The term "hydrogenation of CO_2" is frequently used in this review and elsewhere, but such reactions in basic aqueous solutions may utilize HCO_3^- or CO_3^{2-} depending on the pH of the solution. Formate/formic acid can be used not only for fuel cells, but also as an H_2 storage medium. While formic acid is not the perfect H_2 storage medium (its principal drawback being that it stores only 4.35 wt% of H_2), many researchers consider it better than other methods at this time since the conversion of CO_2 and formic acid can take place cleanly to form H_2 without detectable CO under mild conditions. In addition, formic acid is used as a preservative, insecticide, and industrial material for synthetic processes [4,6,9]. We recently found that the role of pendent base(s) in the second coordination sphere is important for efficient CO_2 hydrogenation [6,10] as found in biological systems. For example, based on the structure of Fe–Fe hydrogenases [11], H_2 activation (i.e., the Fe center accepting a hydride and a pendent nitrogen base accepting a proton) has been proposed to occur via addition of H_2 to a metal center followed by heterolytic cleavage of the bound H_2 (Scheme 1) [12,13]. Various bio-inspired model complexes have been developed, and an advantageous effect of a pendent base has been proved for H_2 oxidation and H_2 production [14–20].

Recently Crabtree published an excellent review on ligand design with additional functional groups such as proton responsive ligands capable of gaining or losing one or more protons, ligands having a hydrogen bonding function, electroresponsive ligands capable of gaining or losing one or more electrons, and photoresponsive ligands capable of undergoing a useful change in properties upon irradiation [21]. Biological systems cleverly use proton responsive ligands, hydrogen bonding interactions and pendent bases in the second coordination sphere. Here we explain how biological inspirations help us to design homogeneous transition-metal catalysts for carrying out the interconversion of CO_2 and formate under ambient conditions in environmentally benign and economically desirable water solvent. By reviewing the results of CO_2 hydrogenation using our catalysts and catalysts from other published studies, we hope to demonstrate a new design principle that greatly improves the catalytic activity.

2. Hydrogenation of CO_2

Hydrogenation of CO_2 to formic acid is a promising way to utilize CO_2 because carbon dioxide is an abundant and inexpensive C1 source. Hydrogenation of CO_2 has been extensively investigated using transition-metal complexes, especially with rhodium, ruthenium, and iridium metal centers in organic solvents, super critical CO_2 ($scCO_2$) and water, typically with bases such as amines, bicarbonates, carbonates and hydroxides [22]. While the reaction in the aqueous phase is exergonic with an added base, the reactions were typically carried out at high temperature and pressure as seen in Table 1. However, the identification of a new bio-inspired design principle for CO_2 hydrogenation catalysts has opened the door for carrying out the reaction at ambient temperature and pressure [6,10]. We first summarize some pioneering work illustrating how this field has developed.

2.1. Metal catalysts with phosphine ligands

Based on the early discovery by Inoue et al. in 1976 [23] that $RuH_2(PPh_3)_4$ catalyzes CO_2 hydrogenation under high pressures of CO_2 and H_2 at room temperature in wet benzene containing NEt_3, Jessop et al. used $scCO_2$ in order to obtain a high turnover frequency (TOF). They found that the use of $scCO_2$ dramatically improved the $RuH_2(PMe_3)_4$- or $RuCl_2(PMe_3)_4$-catalyzed hydrogenation of CO_2 with a very high initial rate of ≥4000 moles of formic acid per mole of catalyst per hour at 50 °C and 8.0–8.5 MPa of H_2 as shown in Table 1 [24,25]. Using a simple high-pressure apparatus, $scCO_2$ is accessible and has many advantages as a solvent: high concentration of CO_2; high miscibility with H_2; good mass-transport capability; tunability of physical properties (e.g., viscosity, dielectric constant, etc.) as a function of temperature and pressure, with particularly dramatic effects being observed near the critical point; and ease of separation of products. Jessop and coworkers further improved the CO_2 hydrogenation catalyzed by $RuCl(OAc)(PMe_3)_4$ with C_6F_5OH and NEt_3 in $scCO_2$ and obtained the remarkably high TOF of 95,000 h^{-1} at 50 °C and 7.0 MPa of H_2 [26].

Basic water can be a solvent for the hydrogenation of CO_2; Joó and coworkers extensively investigated the hydrogenation of CO_2 in basic aqueous solution with rhodium and ruthenium complexes with water soluble phosphine ligands [27–31]. When $[RuCl_2(TPPMS)_2]_2$ (TPPMS = *meta*-monosulfonated triphenylphosphine) is used as a catalyst in an aqueous solution containing 0.3 M $NaHCO_3$ at 80 °C, $P(H_2) = 6.0$ MPa and $P(CO_2) = 3.5$ MPa, they obtained the remarkably high TOF value of 9600 h^{-1} [32].

To understand the factors that control the catalytic activity of CO_2 hydrogenation, Jessop and coworkers investigated the correlations among the catalytic activities of ruthenium catalysts containing 44 different phosphine ligands and properties of the phosphine ligands in $MeOH/N^iPr_3$ [33]. They found that there was no clear correlation between the electronic factors (basicity, Hammett constant, etc.) of monophosphines (PR_3) and the activity of the catalysts comprising them. (This is in marked contrast to what Himeda found for Cp*Ir bipyridine derivatives [5] as we will discuss below.) On the other hand, weakly basic diphosphines

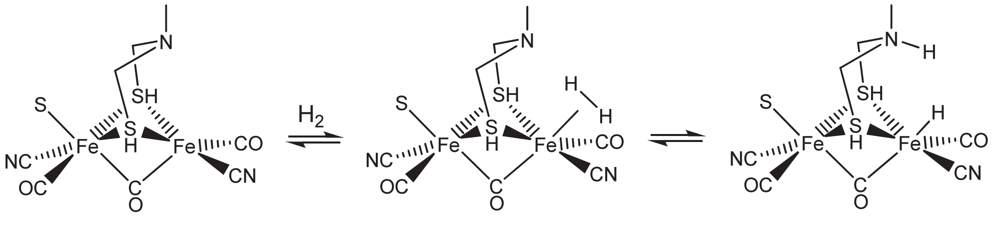

Scheme 1. Proposed mechanism of H_2 production and oxidation by Fe–Fe hydrogenases.

Table 1
Some examples of catalytic systems for the hydrogenation of CO_2 to formic acid.

Complex	Solvent	Additives	p (H_2) MPa	p (CO_2) MPa	T (°C)	T, h	TOF, h^{-1}	TON	Reference
$RuH_2(PPh_3)_4$	C_6H_6	NEt_3, H_2O	2.5	2.5	RT	20	4	87	[23]
$RuH_2(PMe_3)_4$	$scCO_2$	NEt_3, H_2O	8.5	12.0	50	1	1400	1400	[24,25]
$RuCl(OAc)(PMe_3)_4$	$scCO_2$	NEt_3, C_6F_5OH	7.0	12.0	50	0.3	95,000	32,000	[26]
$[RuCl_2(TPPMS)_2]_2$ [a]	H_2O	$NaHCO_3$	6.0	3.5	80	0.03	9600	320	[32]
$RuCl_2(C_6H_6)_2$/dppm[b]	H_2O, THF	$NaHCO_3$	8.0	0	70	20	55	1100	[42]
$Fe(BF_4)_2/PP_3$[c]	MeOH	$NaHCO_3$	6.0	0	80	20	30	610	[34]
$Co(BF_4)_2/PP_3$	MeOH	$NaHCO_3$	6.0	0	120	20	200	3900	[35]
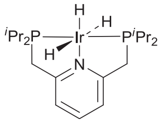	H_2O, THF	KOH	4.0	4.0	200	2	150,000	300,000	[36,37]
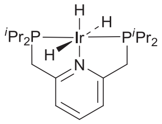	H_2O, THF	KOH	4.0	4.0	120	48	73,000	3,500,000	[36,37]
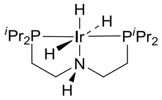	H_2O	KOH	2.8	2.8	185	24	14,500	348,000	[41]
$[Cp^*Ir(4,4'\text{-}(MeO)_2\text{-}bpy)(H_2O)]^{2+}$	H_2O	Citrate, pH 3	5.5	2.5	40	0.5	27	–	[43]
$[Cp^*Ir(bpy)Cl]^{+}$[d]	H_2O	1 M KOH	2	2	80	20	6	105	[44]
$[Cp^*Ir(bpy)Cl]^{+}$[d]	H_2O	KOH	0.05	0.05	25			0	[44]
$[Cp^*Ir(4DHBP)Cl]^{+}$[d]	H_2O	1 M KOH	3	3	120	57	42,000	190,000	[45]
$[Cp^*Ir(4DHBP)Cl]^{+}$[d]	H_2O	1 M KOH	2	2	80	20	7960	6770	[44]
$Cp^*Ir(4DHBP)(H_2O)^{2+}$	H_2O	1 M $NaHCO_3$	0.05	0.05	25	24	7	92	[6]
$[Cp^*Ir(DHPT)Cl]^{+}$[d]	H_2O	1 M KOH	3	3	120	48	33,000	222,000	[45]
$[Cp^*Ir(DHPT)Cl]^{+}$[d]	H_2O	0.1 M K_2CO_3	0.05	0.05	30	30	3.5	81	[45]
$[Cp^*IrCl]_2$ $(THBPM)^{2+}$[d]	H_2O	1 M $NaHCO_3$	0.05	0.05	25	336	64	7200	[6]
$[Cp^*IrCl]_2$ $(THBPM)^{2+}$[d]	H_2O	2 M $KHCO_3$	0.05	0.05	25	216	70	2230	[6]
$[Cp^*IrCl]_2$ $(THBPM)^{2+}$[d]	H_2O	2 M $KHCO_3$	2.5	2.5	80	2	54,000	79,000	[6]
$Cp^*Ir(6DHBP)(H_2O)^{2+}$	H_2O	1 M $NaHCO_3$	0.5	0.5	120	8	25,000	13,000	[10]
$Cp^*Ir(6DHBP)(H_2O)^{2+}$	H_2O	1 M $NaHCO_3$	0.05	0.05	25	33	27	330	[10]
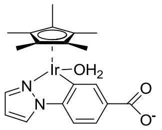	H_2O	2.2 M $K_2CO_3/KHCO_3$	0.05	0.05	30	15	6.8	>100	[46]

[a] TPPMS = sodium diphenylphosphinobenzene-3-sulfonate.

[b] dppm = 1,2-bis(diphenylphosphino)methane.

[c] PP_3 = P(CH2CH2PPh2)3.

[d] Under the reaction conditions, the parent Cl catalyst converts to the aqua species.

(i.e., bis(diphenylphosphino)-based ligands) formed highly active catalysts only if their bite angles were small, while more strongly basic diphosphines (i.e., bis(dicyclohexylphosphino)-based ligands) had the opposite trend.

Beller et al. recently discovered an active iron catalyst system consisting of $Fe(BF_4)_2$ and a tetradentate ligand $P(CH_2CH_2PPh_2)_3$, PP_3, for the reduction of both carbon dioxide and bicarbonates to give formates, alkyl formates (with added corresponding alcohol), and formamides (with added MeOH and the corresponding amine) [34]. The active catalysts in this system were identified as $[FeH(PP_3)]BF_4$ and $[Fe(H)(H_2)(PP_3)]BF_4$. The use of the analogous cobalt system for the hydrogenation of bicarbonate and CO_2, where the active catalyst is $[Co(H_2)PP_3]^+$, significantly improved the turnover number (TON) and TOF as shown in Table 1. It is noteworthy that these non-precious-metal catalyst systems have become competitive with many known precious-metal systems for the hydrogenation of CO_2 [35].

2.2. IrPNP complexes with/without secondary coordination sphere interactions

Nozaki and coworkers used the Ir pincer complex, $Ir(PNP)H_3$ bearing isopropyl groups on the phosphorus atoms (PNP = 2, 6-$(CH_2P^iPr_2)_2$-C_5H_3N, see structure in Table 1), for CO_2 hydrogenation in 1 M KOH solution containing THF as co-solvent owing to the catalyst's limited solubility [36]. The system exhibited higher TON (3.5×10^6 at 120 °C) and TOF (1.5×10^5 h^{-1} at 200 °C) than reported for any other catalyst to date (Table 1). Since they adjusted the total pressure (6.0 and 5.0 MPa, respectively, for experiments at the two final temperatures) at room temperature, the actual pressure under experimental conditions was later reported to be about 8.0 MPa [37]. Interestingly, this catalyst does not produce formate at 25 °C even at high pressure (5.0 MPa). They proposed a catalytic cycle consisting of iridium trihydride **a**, iridium formate **b**, and coordinatively unsaturated amidoiridium dihydride **c** intermediates (Scheme 2) on the basis of their experiments. The authors concluded that the unprecedentedly high catalytic activity of the $Ir(PNP)H_3$ catalyst (**a**, R ^{i}Pr) is possibly due to the acceleration of formate dissociation from **b** mediated by the deprotonation of the ligand [36].

In order to fully understand the mechanism of this highly active system, several theoretical groups have investigated reaction pathways and energetics using density functional theory (DFT) [37–40]. A detailed analysis of the mechanism was performed in a collaboration between the Nozaki and Morokuma groups [37] comparing experimental results with DFT calculations of free-energy profiles of possible pathways. They confirmed that the pathway previously suggested by Nozaki [36] via the deprotonative dearomatization

Table 2
Some examples of catalytic systems for the dehydrogenation of formic acid.

Complex	Solvent	Additives	*T* (°C)	CO detected	TOF, h^{-1}	TON	Reference
$[RuCl_2(C_6H_6)]$/dppm[a]	DMF,H_2O	HCO_2Na	60	<1 ppm	2592	>2000	[42]
$[RuCl_2(C_6H_6)]$/dppe[b]	$HexNMe_2$		25	–	900	260,000	[59]
$[RuCl_2(TPPMS)_2]_2$ [c]	H_2O		80		120		[62]
$Fe(BF_4)_2/PP_3$[d]	PC[d]		80	no.	5,390	92,400	[61]
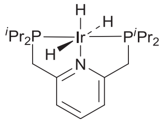	H_2O		60	–	20	890	[37]
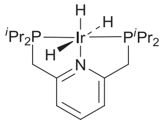	^tBuOH	Et_3N	80	–	120,000	2000	[37]
Cp*Ir(4,4′-MeO-bpy)$(H_2O)^{2+}$[e]	H_2O		60	no	1200		[49]
Cp*Ir(bpy)$(H_2O)^{2+}$[e]	H_2O		60	no	30		[49]
Cp*Ir(4DHBP)$(H_2O)^{2+}$[e]	H_2O		90	no	14,000	10,000	[49]
Cp*Ir(4DHBP)$(H_2O)^{2+}$[e]	H_2O		60	no	2400	10,000	[49]
$[Cp^*IrCl]_2(THBPM)^{2+}$ [fg]	H_2O	HCO_2Na	80	no	158,000	308,000	[6]
$[Cp^*IrCl]_2(THBPM)^{2+}$[fg]	H_2O	HCO_2Na	90	no	228,000	165,000	[6]
Cp*Ir(6DHBP)$(H_2O)^{2+}$[g]	H_2O	HCO_2Na	60	no	6000	5300	[h]
Cp*Ir(6DHBP)$(H_2O)^{2+}$[e]	H_2O		60	no	2400	10,000	[h]
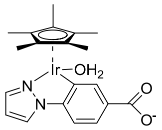	H_2O	HCO_2K	25	no	1,880	>250	[46]

[a] no HCOOH used, dppm = 1,2-bis(diphenylphosphino)methane.
[b] dppe = 1,2-bis(diphenylphosphino)ethane.
[c] TPPMS = sodium diphenylphosphinobenzene-3-sulfonate.
[d] $PP_3 = P(CH_2CH_2PPh_2)_3$, PC = propylene carbonate.
[e] HCOOH pH 1.7.
[f] Under the reaction conditions, the parent Cl catalyst converts to the aqua species.
[g] pH 3.5.
[h] unpublished result.

of the pyridine ring of the hydroxodihydride complex as the rate-determining step is energetically viable and should be strongly affected by the concentration of base. It does not, however, account for the strong dependence on H_2 pressure observed experimentally. They also found that the alternative mechanism proposed by Ahlquist [38] and by Yang [40] involving the hydrogenolysis of the dihydride complex as the rate-determining step has a similar energetic barrier, and should have a strong dependence on hydrogen pressure. Moreover, neither mechanism alone can account for the observed kinetic isotope effect in D_2O solvent. They suggested that the two mechanisms probably compete, and that both contribute to the overall reaction.

Hazari and coworkers have theoretically investigated CO_2 insertion into an Ir—H bond for Ir(PNP′)H_2X (where X = H, Ph, Me, OH, Cl and I, PNP′ = 2, 6–$(CH_2PMe_2)_2$-C_5H_3N, similar to Nozaki's catalyst, but bearing methyl groups on the phosphorus atoms) and found that CO_2 insertion is thermodynamically unfavorable in THF at room temperature under 1 atm CO_2 [41]. Their DFT calculations predict that Ir(PN^HP)H_3 (PN^HP = HN($^iPr_2PC_2H_4$)$_2$, which has an H-bond donor in the secondary coordination sphere (compound **d** in Scheme 2), favorably inserts CO_2 into the Ir—H bond. They isolated the air stable formate complex **e** and characterized it by X-ray diffraction. The insertion of CO_2 is reversible and the exposure of **e** to 1 atm $^{13}CO_2$ at room temperature resulted in rapid incorporation of ^{13}C into

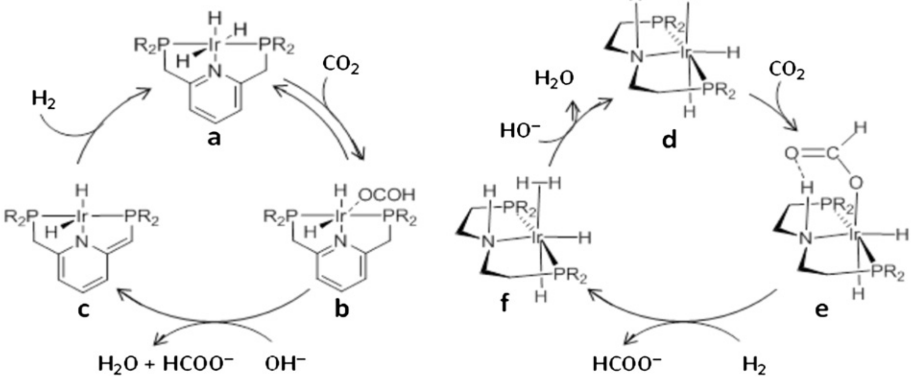

Scheme 2. Proposed mechanisms for CO_2 hydrogenation by Ir(PNP)H_3 and Ir(PN^HP)H_3.

the formate complex. The formate complex catalyzed CO_2 hydrogenation in 1 M KOH with a maximal TON and TOF of 348,000 and 18,780 h^{-1}, respectively, at 185 °C and 5.5 MPa ($H_2/CO_2 = 1$), however, these values are smaller than those obtained with Ir(PNP)H_3. The proposed mechanism for the Ir(PN^{H}P)H_3 catalytic system, shown in Scheme 2, involves facile CO_2 insertion using a second coordination sphere effect of the NH of the PN^{H}P ligand, followed by formate displacement by H_2 as the rate-determining step, not hydrogenolysis of the dihydride complex as one of two possible rate-determining steps as proposed for the case of Ir(PNP)H_3 [37]. Loss of the formate ligand should not be difficult in aqueous solution, but may be considerably endergonic in organic solvent or the gas phase. While the authors could not rule out the deprotonation of the amine linker to convert **e** into an amido species, and subsequent release of formate, such a step might be important for designing a more active system considering the highly active Ir(PNP)H_3 case. However, no clear advantages of an H-bond donor in the secondary coordination sphere were observed in the catalytic rate, indicating that such an H-bonded interaction is not likely to be involved in the rate determining step, in contrast to our finding using Cp*Ir bipyridine derivatives [10] as discussed below.

2.3. IrCp* complexes with proton-responsive ligands

Himeda and coworkers have introduced the new concept of proton responsive ligands capable of losing one or more protons in basic media and promoting a higher catalytic activity via producing more electron donating ligands in metal complexes for CO_2 hydrogenation. The first such complexes were [Cp*IrCl(4DHBP)]$^+$ (Cp* η^5-C_5Me_5, 4DHBP 4,4′-dihydroxy-2,2′-bipyridine) and [Cp*IrCl(DHPT)]$^+$ (DHPT 4,7-dihydroxy-1,10-phenanthroline) [44,45,47–49]. These complexes aquate rapidly in water to form the corresponding aqua species, [Cp*Ir(4DHBP)(OH_2)]$^{2+}$ (and [Cp*Ir(DHPT)(OH_2)]$^{2+}$), which deprotonate in neutral and basic media as shown in Scheme 3. Spectroscopic titration indicates pK_as of the 4DHBP and the bound H_2O are 5 (average value) and 9.6, respectively, for [Cp*Ir(4DHBP)(OH_2)]$^{2+}$.

The aqua complex [Cp*Ir(4,4′-(MeO)$_2$-bpy)(OH_2)]$^{2+}$ ((4,4′-MeO)$_2$-bpy 4,4′-dimethoxy-2,2′-bipyridine) remarkably catalyzes formic acid generation via CO_2 hydrogenation in an acidic aqueous solution (pH 3) at 40 °C and high pressure of CO_2 and H_2 [43]. However, when [Cp*Ir(4DHBP)(OH_2)]$^{2+}$ and [Cp*Ir(DHPT)(OH_2)]$^{2+}$ that have the ‘multifunctional’ phenolic ligands are used as catalysts and these ligands are deprotonated in basic solution, the catalysts are activated and their catalytic activities for CO_2 hydrogenation significantly improve. They produce formate even at room temperature under atmospheric pressure (i.e., 0.5 atm H_2 and 0.5 atm CO_2) [50]. These remarkable results are shown in Table 1. It should also be noted that [Cp*Ir(DHPT)(OH_2)]$^{2+}$ has an additional attractive property. At the end of the CO_2-hydrogenation reaction (resulting in a decrease of the pH in the solution), the catalyst can be precipitated because of its low solubility in weak acidic solution such as pH 5.5. Therefore the catalyst can be recycled and the product is easy to separate [48]. Furthermore, preparing the related species with bpy (Hammett's constant for –H: $\sigma_p^+ = 0$), 4,4′-(CO_2^-)$_2$-bpy (−CO_2^-: $\sigma_p^+ = -0.02$), 4,4′-Me_2-bpy (−Me: $\sigma_p^+ = -0.31$), and 4,4′-(OMe)$_2$-bpy (−OMe: $\sigma_p^+ = -0.78$) and comparing their catalytic activities to that of the 4DHBP (−OH: $\sigma_p^+ = -0.92$; –O^-: $\sigma_p^+ = -2.32$) complex, Himeda and coworkers have demonstrated a clear correlation between initial catalytic rate and the electronic effect based on Hammett's rule (Fig. 1) [44]. [Cp*Ir(4DHBP)(OH_2)]$^{2+}$, which has the highest electron donating (oxy-anion) ligand in basic solution, showed 1300 times greater catalytic activity for CO_2 hydrogenation than [Cp*Ir(bpy)(OH_2)]$^{2+}$ under the same conditions [44].

Fukuzumi and coworkers recently reported CO_2 hydrogenation at ambient temperature and pressure using a [C,N] cyclometalated complex, [Cp*Ir(4-(1H-pyrazol-1-yl-κN_2)benzoic acid-κC^3)(H_2O)]$_2$ SO_4 [46]. This complex with the proton-responsive benzoic acid functionality releases protons from the carboxyl group (pK_a = 4.0) and the aqua ligand (pK_a 9.5) as shown in Scheme 4. For CO_2 hydrogenation they observed TOFs 6.8 h^{-1} and 22.1 h^{-1} at 30 °C and 60 °C, respectively, at pH 7.5 under 1 atm H_2/CO_2 (v/v = 1).

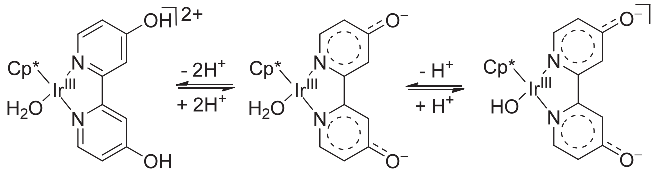

Scheme 3. Acid–base equilibrium between hydroxyl and oxyanion form of [Cp*Ir(4DHBP)(OH_2)]$^{2+}$.

2.4. IrCp* complexes with pendent bases in the secondary coordination sphere

While [Cp*Ir(4DHBP)(OH_2)]$^{2+}$ shows excellent catalytic activity for formate production compared to [Cp*Ir(bpy)(OH_2)]$^{2+}$, we sought to further improve that catalyst. In biological systems, enzymes efficiently utilize hydrogen-bonding and acid/base interactions in the secondary coordination sphere in order to carry out multi-electron, proton-coupled reactions. Therefore, we designed a catalyst that has the combined effects of electronic activation via deprotonation of phenolic OH and a pendent base in the secondary coordination sphere as well as iridium center(s) to facilitate the binding of H_2, CO_2, H^+, HCOOH, etc. at the primary coordination site (Scheme 5). Using 4,4′,6,6′-tetrahydroxybipyrimidine (THBPM), we isolated a dinuclear Ir complex [Cp*Ir(Cl)]$_2$(THBPM)Cl_2 and characterized it by X-ray diffraction [6]. The Cl complex readily aquates in water and acts as a catalyst for CO_2 hydrogenation under mild conditions with unprecedented rates in slightly basic solution (pH 8.3). When using a 1:1H_2:CO_2 gas mixture at 0.1 MPa and 25 °C, [Cp*Ir(OH_2)]$_2$(THBPM)$^{4+}$ (Note that the active catalyst is deprotonated.), a turnover frequency (TOF) of 64 h^{-1} and TON of 7,200 were achieved, and yielded 0.36 M formate. Rates and turnovers were increased to a TOF of 53,800 h^{-1} and TON of 153,000 under pressurized conditions at relatively low temperature (see Table 1). The formate concentration reached up to 1.7 M [6]. DFT calculations predict that the deprotonated species has Ir(I) character with a vacant coordination site (i.e., the aqua ligand is lost upon deprotonation, Scheme 5). Facile heterolysis of H_2 with the aid of the pendent base to accept a proton from it may be an indispensable pathway for forming the Ir—H species, which we believe to be the

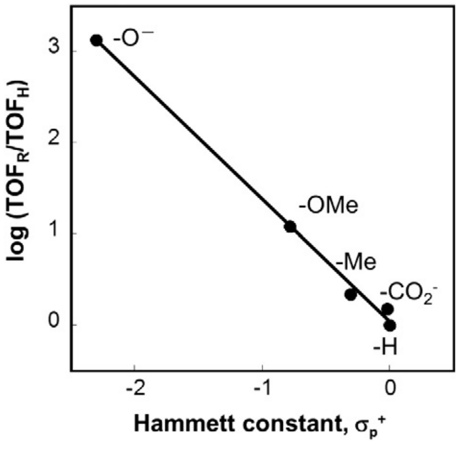

Fig. 1. Hammett plots of CO_2 hydrogenation. Reaction conditions: 4 MPa H_2/CO_2 (1/1), 80 °C.

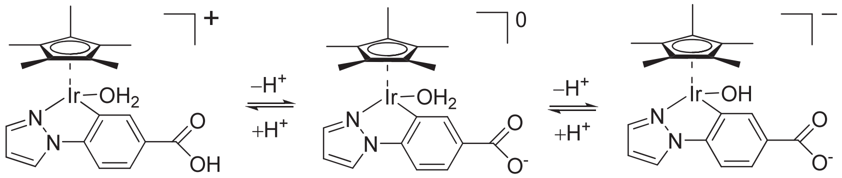

Scheme 4. Acid–base equilibrium of iridium aqua complexes.

rate-determining step. We expect CO_2 insertion into the Ir—H bond to be rather fast by comparison.

In order to systematically examine the multifunctional ligand effects in more detail and understand the mechanism of CO_2 hydrogenation, we have synthesized the mononuclear species [Cp*Ir(6,6′-R_2-bpy)(OH_2)] SO_4 (R = OH, OMe, Me), which have varied donor powers at the 6 and 6′ positions on bpy. As with the [Cp*Ir(4,4′-R_2-bpy)(OH_2)] SO_4 species, a good correlation between the ligand substituents' Hammett parameters and initial catalytic rates for CO_2 hydrogenation was observed. An *additional* rate enhancement (∼4 times under identical conditions) of the catalytic formate generation rate was observed when the OH groups are moved from 4,4′ positions to 6,6′ positions on 2,2′-bipyridine to introduce pendent bases into the secondary coordination sphere [10]. Furthermore, our NMR experiments indicate that $[Cp^*Ir(OH_2)]_2(THBPM)^{4+}$ and $[Cp^*Ir(6DHBP)(OH_2)]^{2+}$ (6DHBP 6,6′-dehydroxy-2,2′-bipyridine) are more facile for formation of Ir–H than $[Cp^*Ir(4DHBP)(OH_2)]^{2+}$. For example, while only 90% of $[Cp^*Ir(4DHBP)(OH_2)]^{2+}$ was converted to Ir–H after 40 h under 0.5 MPa H_2, remarkably 95% of $[Cp^*Ir(6DHBP)(OH_2)]^{2+}$ was converted to Ir–H after 30 minutes under 0.2 MPa H_2. These experimental results match well with DFT calculations at pH 8.3 shown in Fig. 2. According to the calculations with $[Cp^*Ir(6DHBP)(OH_2)]^{2+}$, the free energy barrier is 52.5 kJ mol^{-1}, and H_2 addition through heterolytic cleavage with the "proton relay" involving the pendent base is rate limiting. Our calculations also suggest that CO_2 insertion into the Ir—H bond is stabilized by a weak hydrogen bonding interaction (3.127 Å) with the deprotonated pendent base as shown in the transition-state complex E. Neither insertion of CO_2 nor dissociation of formate is the rate determining step under basic conditions for $[Cp^*Ir(6DHBP)(OH_2)]^{2+}$.

3. Dehydrogenation of formic acid

Formic acid generally decomposes by one of two pathways, into either a mixture of CO_2 and H_2 or into a mixture of CO and H_2O. The former decomposition pathway is particularly desirable because it allows formic acid to act as a hydrogen storage medium. While numerous homogeneous and heterogeneous transition metal catalysts decompose formic acid to CO_2 and H_2 [51–58], we will summarize only complexes that also act as CO_2 hydrogenation catalysts that were discussed above.

While *in situ* generated catalyst from $RuCl_2(C_6H_6)$ and 1,2-bis(diphenylphosphino)methane can decompose HCO_2Na in a mixed solvent of DMF and H_2O [42] (Table 2), Beller and coworkers improved the system by using a continuous mode, and created a highly active and stable system that gave a total TON of approximately 260,000 with average TOF of about 900 h^{-1} to produce H_2 from formic acid at room temperature [59]. They have recently obtained a TON of 800,000 using a similar system with 1,2-bis(diphenylphosphino)ethane [60]. They also reported that an *in situ* produced iron complex from $Fe(BF_4)_2$ and PP_3 catalyzed formic acid dehydrogenation with a high TOF of 9425 h^{-1} and a TON as high as 92,000 in propylene carbonate at 80 °C [61]. DFT calculations predict two competing pathways involving $Fe(PP_3)H$ as a common key intermediate for H_2 generation. In both pathways the ß-hydride elimination of CO_2 from the bound formate is considered to be the rate-determining step [61].

The highly active CO_2 hydrogenation catalyst $IrPNP(H)_3$ investigated by Nozaki and coworkers is a rather poor catalyst for dehydrogenation of formic acid in water or with NaOH [37]. However the use ^{t}BuOH as the solvent in addition to Et_3N as a base enhanced the catalytic activity to an initial TOF of 120,000 h^{-1}.

$Cp^*Ir(L)(H_2O)^{2+}$ (L = 4,4′-R_2-bpy, R = H, Me, OMe, and OH) and $[Cp^*Ir(OH_2)]_2(THBPM)^{4+}$ all show catalytic activity for formic acid decomposition to H_2 and CO_2 without forming CO. A remarkable improvement was observed by using 4DHBP (R = OH) instead of bpy (R = H). Furthermore, a clear correlation was observed between initial TOFs and Hammett σ_p^+ values of the substituents of 4,4′-R_2-bpy (R = H, Me, OMe, OH) in 1 M aq. formic acid solution at 60 °C [49]. While a dinuclear complex with a THBPM ligand is an excellent catalyst for CO_2 hydrogenation even at ambient conditions, it also had the highest observed activity for formic acid decomposition in aqueous solution containing a 1:1 mixture of HCO_2H and HCO_2Na: TOF 228,000 at 90 °C; TON 308,000 at 80 °C [6]. Interestingly, the investigation on rates of H_2 evolution as a function of pH at 60 °C indicates the rate peaks at 31,600 h^{-1} at pH 3.5, which is close to the average pK_a of the catalyst (3.8) and to the pK_a of formic acid (3.75).

In the case of $[Cp^*Ir(OH_2)]_2(THBPM)^{4+}$, we believe the dependence of the favored direction of the reaction is the key to understanding the dehydrogenation mechanism. With at least half of the –O groups on the ligand protonated, the resonance structures contributing to Ir(I) character of the metal center are far less important, and the metal center becomes less electron rich. This makes formate binding stronger. We envision a β-hydride elimination-like transition state of the Ir formate complex similar to that proposed by Beller et al. [61] and Fukuzumi et al. [46], and think it likely that such a transition state would eliminate CO_2 while the resulting metal hydride would react with a proton from the acidic aqueous solution to form H_2. The main point is that since the forward and

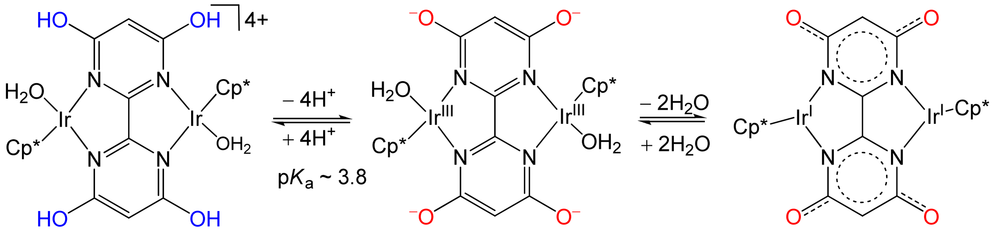

Scheme 5. Reversible removal of protons and the DFT predicted coordinatively unsaturated Ir(I) species (far right).

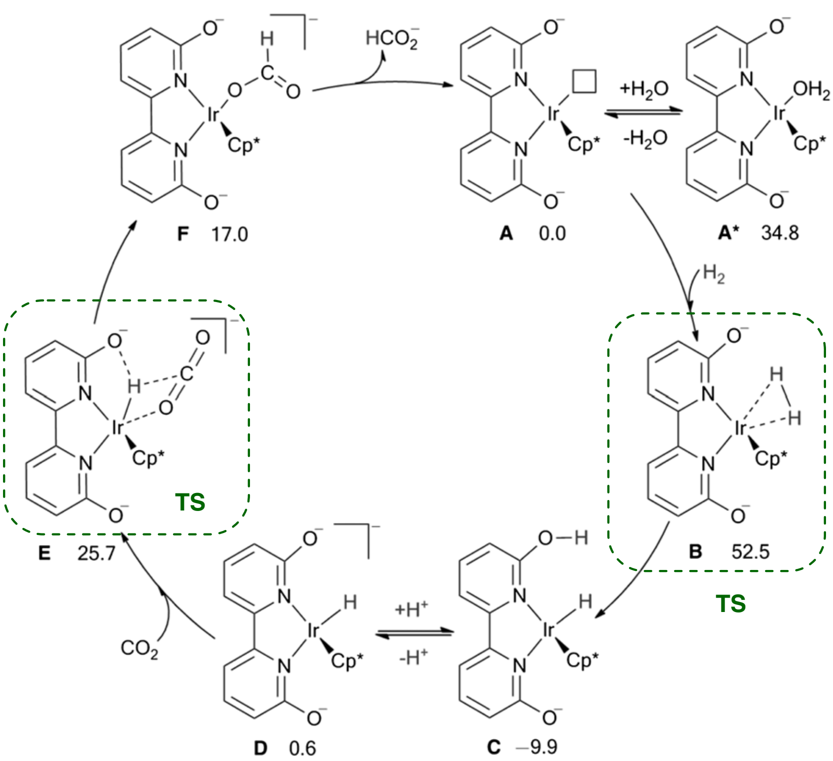

Fig. 2. Proposed mechanism for the hydrogenation of CO_2 by $[Cp^*Ir(6DHBP)(OH_2)]^{2+}$. Computed free energies at pH 8.3 are indicated in units of kJ mol^{-1} relative to 1 M **A** in aqueous solution and 1 atm H_2 and CO_2 gases. **B** and **E** are transition-state species.

reverse reactions of CO_2 hydrogenation are catalyzed by these complexes with proton-active ligands at different pH conditions, the forward and reverse mechanisms have different rate-determining steps.

Fukuzumi and coworkers also recently reported that the interconversion between H_2 and formic acid in water at ambient temperature and pressure has been achieved by using a [C,N] cyclometalated complex, $[Cp^*Ir(4\text{-}(1H\text{-pyrazol-1-yl-}\kappa N_2)\text{benzoic acid-}\kappa C^3)(H_2O)]^+$ [46]. The pH dependence of TOF showed that the maximum TOF value 1880 h^{-1} is obtained at pH 2.8 and 298 K with a total concentration of HCO_2H and HCO_2K of 3.3 M. Because the pK_a of this complex is 4.0, this phenomenon is in sharp contrast to that in $[Cp^*Ir(H_2O)]_2(THBPM)^{4+}$. It is reported that a further decrease in pH to less than 2.8 may result in decomposition of the complex $Cp^*Ir[(4\text{-}(1H\text{-pyrazol-1-yl-}\kappa N_2)\text{benzoic acid-}\kappa C^3)H_2O]^+$, and that the benzoic acid complex is more active than the benzoate complex.

4. Conclusion

Hydrogen is an environmentally benign fuel, and can be produced from water using renewable energy. However, H_2 has physical properties that constrain its commercial use as a fuel: low energy density, difficulty to transport, safety issues, etc. Formic acid is a promising chemical as an H_2 storage medium and as a fuel for formate fuel cells. The interconversion of CO_2 and formic acid under mild conditions in water has been recently achieved using Ru and Ir complexes, and even using non-precious metal Fe complexes. Both the TOF and TON have been remarkably improved. Only a few catalysts seem to reflect a bio-inspired design such as the use of proton-responsive ligands, ligands with pendent bases or acids for a second coordination sphere interaction, electroresponsive ligands, and/or ligands having a hydrogen bonding function with a solvent molecule or an added reagent. The most successful catalyst is $[Cp^*Ir(H_2O)]_2(THBPM)^{4+}$ that at least has the first three of these characteristics associated with its bridging ligand. By utilizing the acid/base equiliblium for proton removal, the ligand becomes a strong electron donor resulting in Ir(I) character with a vacant coordination site at each metal center in basic solution. Complemented by DFT calculations, the rates of formate production using the related Ir complexes with and without such functions on the ligand reveal that the rate-determining step for the CO_2 hydrogenation is likely to be the facile H_2 heterolysis assisted by the second coordination sphere interaction of the pendent base. The dehydrogenation of formic acid, owing to the proton-responsive ligands changing character under acidic pH conditions, is likely to occur by a mechanisms with a different rate-determining step.

Acknowledgements

The work at BNL was carried out under contract DE-AC02-98CH10886 with the U.S. Department of Energy and supported by its Division of Chemical Sciences, Geosciences, & Biosciences, Office of Basic Energy Sciences. YH thanks the Japanese Ministry of Economy, Trade, and Industry for financial support.

References

[1] T. Reda, C.M. Plugge, N.J. Abram, J. Hirst, Reversible interconversion of carbon dioxide and formate by an electroactive enzyme, Proc. Natl. Acad. Sci. U. S. A. 105 (2008) 10654–10658.
[2] J.G. Ferry, Formate dehydrogenase, FEMS Microbiol. Rev. 7 (1990) 377–382.
[3] M.J. Romao, Molybdenum and tungsten enzymes: a crystallographic and mechanistic overview, Dalton Trans. (2009) 4053–4068.
[4] S. Fukuzumi, Bioinspired energy conversion systems for hydrogen production and storage, Eur. J. Inorg. Chem. (2008) 1351–1362.
[5] Y. Himeda, S. Miyazawa, T. Hirose, Interconversion between formic acid and H_2/CO_2 using Rhodium and Ruthenium catalysts for CO_2 fixation and H_2 storage, ChemSusChem 4 (2011) 487–493.
[6] J.F. Hull, Y. Himeda, W.-H. Wang, B. Hashiguchi, R. Periana, D.J. Szalda, J.T. Muckerman, E. Fujita, Reversible hydrogen storage using CO_2 and a proton-switchable iridium catalyst in aqueous media under mild temperatures and pressures, Nat. Chem. 4 (2012) 383–388.

[7] W. Leitner, E. Dinjus, F. Gassner, in: B. Cornils, W.A. Herrmann (Eds.), Aqueous Phase Organometallic Catalysis, Concepts and Applications, Wiley-VCH, Weinheim, 1998, p. 486.

[8] P.G. Jessop, F. Joo, C.C. Tai, Recent advances in the homogeneous hydrogenation of carbon dioxide, Coord. Chem. Rev. 248 (2004) 2425–2442.

[9] F. Joo, Breakthroughs in hydrogen storage-formic acid as a sustainable storage material for hydrogen, ChemSusChem 1 (2008) 805–808.

[10] W.-H. Wang, J.F. Hull, J.T. Muckerman, E. Fujita, Y. Himeda, Second-coordination-sphere and electronic effects enhance iridium(III)-catalyzed homogeneous hydrogenation of carbon dioxide in water near ambient temperature and pressure, Energy Environ. Sci. 5 (2012) 7923–7926.

[11] Y. Nicolet, A.L. de Lacey, X. Vernede, V.M. Fernandez, E.C. Hatchikian, J.C. Fontecilla-Camps, Crystallographic and FTIR spectroscopic evidence of changes in Fe coordination upon reduction of the active site of the Fe-only hydrogenase from *Desulfovibrio desulfuricans*, J. Am. Chem. Soc. 123 (2001) 1596–1601.

[12] H.J. Fan, M.B. Hall, A capable bridging ligand for Fe-only hydrogenase: density functional calculations of a low-energy route for heterolytic cleavage and formation of dihydrogen, J. Am. Chem. Soc. 123 (2001) 3828–3829.

[13] C. Greco, M. Bruschi, L. De Gioia, U. Ryde, A QM/MM investigation of the activation and catalytic mechanism of Fe-only hydrogenases, Inorg. Chem. 46 (2007) 5911–5921.

[14] M. Rakowski DuBois, D.L. DuBois, Development of molecular electrocatalysts for CO_2 reduction and H_2 production/oxidation, Acc. Chem. Res. 42 (2009) 1974–1982.

[15] M. Rakowski DuBois, D.L. DuBois, The roles of the first and second coordination spheres in the design of molecular catalysts for H_2 production and oxidation, Chem. Soc. Rev. 38 (2009) 62–72.

[16] F. Gloaguen, T.B. Rauchfuss, Small molecule mimics of hydrogenases: hydrides and redox, Chem. Soc. Rev. 38 (2009) 100–108.

[17] B.E. Barton, M.T. Olsen, T.B. Rauchfuss, Artificial hydrogenases, Curr. Opin. Biotechnol. 21 (2010) 292–297.

[18] J.M. Camara, T.B. Rauchfuss, Mild redox complementation enables H_2 activation by [FeFe]-hydrogenase models, J. Am. Chem. Soc. 133 (2011) 8098–8101.

[19] J.M. Camara, T.B. Rauchfuss, Combining acid–base, redox and substrate binding functionalities to give a complete model for the [FeFe]-hydrogenase, Nat. Chem. 4 (2011) 26–30.

[20] M.Y. Darensbourg, R.D. Bethel, Biomimetic chemistry merging the old with the new, Nat. Chem. 4 (2012) 11–13.

[21] R.H. Crabtree, Multifunctional ligands in transition metal catalysis, New J. Chem. 35 (2011) 18–23.

[22] Y. Himeda, W.-H. Wang, Application of carbon dioxide in hydrogen storage: homogeneous hydrogenation of carbon dioxide and dehydrogenation of formic acid, in: S.L. Suib (Ed.), New and Future Developments in Catalysis. Activation of Carbon Dioxide, Elsevier Inc., Philadelphia, in press.

[23] Y. Inoue, H. Izumida, Y. Sasaki, H. Hashimoto, Catalytic fixation of carbon dioxide to formic acid by transition-metal complexes under mild conditions, Chem. Lett. (1976) 863–864.

[24] P.G. Jessop, T. Ikariya, R. Noyori, Homogeneous catalytic hydrogenation of supercritical carbon dioxide, Nature 368 (1994) 231–233.

[25] P.G. Jessop, Y. Hsiao, T. Ikariya, R. Noyori, Homogeneous catalysis in supercritical fluids: hydrogenation of supercritical carbon dioxide to formic acid, alkyl formates, and formamides, J. Am. Chem. Soc. 118 (1996) 344–355.

[26] P. Munshi, A.D. Main, J.C. Linehan, C.C. Tai, P.G. Jessop, Hydrogenation of carbon dioxide catalyzed by ruthenium trimethylphosphine complexes: the accelerating effect of certain alcohols and amines, J. Am. Chem. Soc. 124 (2002) 7963–7971.

[27] F. Joo, G. Laurenczy, L. Nadasdi, J. Elek, Homogeneous hydrogenation of aqueous hydrogen carbonate to formate under exceedingly mild conditions — a novel possibility of carbon dioxide activation, Chem. Commun. (1999) 971–972.

[28] F. Joo, G. Laurenczy, P. Karady, J. Elek, L. Nadasdi, R. Roulet, Homogeneous hydrogenation of aqueous hydrogen carbonate to formate under mild conditions with water soluble rhodium(I)- and ruthenium(II)-phosphine catalysts, Appl. Organomet. Chem. 14 (2000) 857–859.

[29] I. Joszai, F. Joo, Hydrogenation of aqueous mixtures of calcium carbonate and carbon dioxide using a water-soluble rhodium(I)-tertiary phosphine complex catalyst, J. Mol. Catal. A Chem. 224 (2004) 87–91.

[30] A. Katho, Z. Opre, G. Laurenczy, F. Joo, Water-soluble analogs of $[RuCl_3(NO)(PPh_3)_2]$ and their catalytic activity in the hydrogenation of carbon dioxide and bicarbonate in aqueous solution, J. Mol. Catal. A Chem. 204 (2003) 143–148.

[31] G.Y. Zhao, F. Joo, Free formic acid by hydrogenation of carbon dioxide in sodium formate solutions, Catal. Commun. 14 (2011) 74–76.

[32] J. Elek, L. Nadasdi, G. Papp, G. Laurenczy, F. Joo, Homogeneous hydrogenation of carbon dioxide and bicarbonate in aqueous solution catalyzed by water-soluble ruthenium(II) phosphine complexes, Appl. Catal. A 255 (2003) 59–67.

[33] C.-C. Tai, J. Pitts, J.C. Linehan, A.D. Main, P. Munshi, P.G. Jessop, In situ formation of ruthenium catalysts for the homogeneous hydrogenation of carbon dioxide, Inorg. Chem. 41 (2002) 1606–1614.

[34] C. Federsel, A. Boddien, R. Jackstell, R. Jennerjahn, P.J. Dyson, R. Scopelliti, G. Laurenczy, M. Beller, A well-defined iron catalyst for the reduction of bicarbonates and carbon dioxide to formates, alkyl formates, and formamides, Angew. Chem. Int. Ed. 49 (2010) 9777–9780.

[35] C. Federsel, C. Ziebart, R. Jackstell, W. Baumann, M. Beller, Catalytic hydrogenation of carbon dioxide and bicarbonates with a well-defined cobalt dihydrogen complex, Chem. Eur. J. 18 (2012) 72–75.

[36] R. Tanaka, M. Yamashita, K. Nozaki, Catalytic hydrogenation of carbon dioxide using Ir(III)-pincer complexes, J. Am. Chem. Soc. 131 (2009) 14168–14169.

[37] R. Tanaka, M. Yamashita, L.W. Chung, K. Morokuma, K. Nozaki, Mechanistic studies on the reversible hydrogenation of carbon dioxide catalyzed by an Ir-PNP complex, Organometallics 30 (2011) 6742.

[38] M.S.G. Ahlquist, Iridium catalyzed hydrogenation of CO_2 under basic conditions—mechanistic insight from theory, J. Mol. Catal. A Chem. 324 (2010) 3–8.

[39] J. Li, K. Yoshizawa, Catalytic hydrogenation of carbon dioxide with a highly active hydride on Ir(III)–Pincer complex: mechanism for CO_2 insertion and nature of metal-hydride bond, Bull. Chem. Soc. Jpn. 84 (2011) 1039–1048.

[40] X.Z. Yang, Hydrogenation of carbon dioxide catalyzed by PNP pincer iridium, iron, and cobalt complexes: a computational design of base metal catalysts, ACS Catal. 1 (2011) 849–854.

[41] T.J. Schmeier, G.E. Dobereiner, R.H. Crabtree, N. Hazari, Secondary coordination sphere interactions facilitate the insertion step in an iridium(III) CO_2 reduction catalyst, J. Am. Chem. Soc. 133 (2011) 9274–9277.

[42] A. Boddien, F. Gartner, C. Federsel, P. Sponholz, D. Mellmann, R. Jackstell, H. Junge, M. Beller, CO_2-“neutral” hydrogen storage based on bicarbonates and formates, Angew. Chem. Int. Ed. 50 (2011) 6411–6414.

[43] S. Ogo, R. Kabe, H. Hayashi, R. Harada, S. Fukuzumi, Mechanistic investigation of CO_2 hydrogenation by Ru(II) and Ir(III) aqua complexes under acidic conditions: two catalytic systems differing in the nature of the rate determining step, Dalton Trans. (2006) 4657–4663.

[44] Y. Himeda, N. Onozawa-Komatsuzaki, H. Sugihara, K. Kasuga, Highly efficient conversion of carbon dioxide catalyzed by half-sandwich complexes with pyridinol ligand: the electronic effect of oxyanion, J. Photochem. Photobiol. A 182 (2006) 306–309.

[45] Y. Himeda, N. Onozawa-Komatsuzaki, H. Sugihara, K. Kasuga, Simultaneous tuning of activity and water solubility of complex catalysts by acid–base equilibrium of ligands for conversion of carbon dioxide, Organometallics 26 (2007) 702–712.

[46] Y. Maenaka, T. Suenobu, S. Fukuzumi, Catalytic interconversion between hydrogen and formic acid at ambient temperature and pressure, Energy Environ. Sci. 5 (2012) 7360–7367.

[47] Y. Himeda, N. Onozawa-Komatsuzaki, H. Sugihara, H. Arakawa, K. Kasuga, Half-sandwich complexes with 4,7-dihydroxy-1,10-phenanthroline: water-soluble, highly efficient catalysts for hydrogenation of bicarbonate attributable to the generation of an oxyanion on the catalyst ligand, Organometallics 23 (2004) 1480–1483.

[48] Y. Himeda, N. Onozawa-Komatsuzaki, H. Sugihara, K. Kasuga, Recyclable catalyst for conversion of carbon dioxide into formate attributable to an oxyanion on the catalyst ligand, J. Am. Chem. Soc. 127 (2005) 13118–13119.

[49] Y. Himeda, Highly efficient hydrogen evolution by decomposition of formic acid using an iridium catalyst with 4,4′-dihydroxy-2,2′-bipyridine, Green Chem. 11 (2009) 2018–2022.

[50] Y. Himeda, Conversion of CO_2 into formate by homogeneously catalyzed hydrogenation in water: tuning catalytic activity and water solubility through the acid–base equilibrium of the ligand, Eur. J. Inorg. Chem. (2007) 3927–3941.

[51] M. Grasemann, G. Laurenczy, Formic acid as a hydrogen source — recent developments and future trends, Energy Environ. Sci. 5 (2012) 8171–8181.

[52] B. Loges, A. Boddien, H. Junge, M. Beller, Controlled generation of hydrogen from formic acid amine adducts at room temperature and application in H_2/O_2 fuel cells, Angew. Chem. Int. Ed. 47 (2008) 3962–3965.

[53] W. Gan, C. Fellay, P.J. Dyson, G. Laurenczy, Influence of water-soluble sulfonated phosphine ligands on ruthenium catalyzed generation of hydrogen from formic acid, J. Coord. Chem. 63 (2010) 2685–2694.

[54] C. Fellay, P.J. Dyson, G. Laurenczy, A viable hydrogen-storage system based on selective formic acid decomposition with a ruthenium catalyst, Angew. Chem. Int. Ed. 47 (2008) 3966–3968.

[55] C. Fellay, N. Yan, P.J. Dyson, G. Laurenczy, Selective formic acid decomposition for high-pressure hydrogen generation: a mechanistic study, Chem. Eur. J. 15 (2009) 3752–3760.

[56] D.J. Morris, G.J. Clarkson, M. Wills, Insights into hydrogen generation from formic acid using ruthenium complexes, Organometallics 28 (2009) 4133–4140.

[57] B. Loges, A. Boddien, F. Gartner, H. Junge, M. Beller, Catalytic generation of hydrogen from formic acid and its derivatives: useful hydrogen storage materials, Top. Catal. 53 (2010) 902–914.

[58] M. Yadav, Q. Xu, Liquid-phase chemical hydrogen storage materials, Energy Environ. Sci. 5 (2012) 9698–9725.

[59] A. Boddien, B. Loges, H. Junge, F. Gartner, J.R. Noyes, M. Beller, Continuous hydrogen generation from formic acid: highly active and stable ruthenium catalysts, Adv. Synth. Catal. 351 (2009) 2517–2520.

[60] A. Boddien, C. Federsel, P. Sponholz, D. Mellmann, R. Jackstell, H. Junge, G. Laurenczy, M. Beller, Toward the development of a hydrogen battery, Energy Environ. Sci. 5 (2012) 8907–8911.

[61] A. Boddien, D. Mellmann, F. Gartner, R. Jackstell, H. Junge, P.J. Dyson, G. Laurenczy, R. Ludwig, M. Beller, Efficient dehydrogenation of formic acid using an iron catalyst, Science 333 (2011) 1733–1736.

[62] G. Papp, J. Csorba, G. Laurenczy, F. Joo, A charge/discharge device for chemical hydrogen storage and generation, Angew. Chem. Int. Ed. 50 (2011) 10433–10435.